Effective Liquid Chromatography – Trapped Ion Mobility Spectrometry – Mass Spectrometry Separation of Isomeric Lipid Species

Kevin Jeanne Dit Fouque,[†] Cesar E. Ramirez,[†] Russell L. Lewis,[‡] Jeremy P. Koelmel,[§] Timothy J. Garrett,[§] Richard A. Yost,[§,‡] and Francisco Fernandez-Lima.*[,†]

[†] Department of Chemistry and Biochemistry, Florida International University, Miami, FL 33199, United States.

[‡] Department of Chemistry, University of Florida, Gainesville, FL 32611, Unites States.

[§] Department of Pathology, Immunology and Laboratory Medicine, University of Florida, Gainesville, FL 32610, United States.

ABSTRACT: Lipids are a major class of molecules that play key roles in different biological processes. Understanding their biological roles and mechanisms remains analytically challenging due to their high isomeric content (e.g., varying acyl chain positions and/or double bond locations/geometries) in eukaryotic cells. In the present work, a combination of liquid chromatography (LC) followed by high resolution trapped ion mobility spectrometry – mass spectrometry (TIMS-MS) was used to investigate common isomeric glycerophosphocholine (PC) and diacylglycerol (DG) lipid species from human plasma. The LC dimension was effective for the separation of isomeric lipid species presenting distinct double bond locations or geometries, but was not able to differentiate lipid isomers with distinct acyl chain positions. High resolution TIMS-MS resulted in the identification of lipid isomers that differ in the double bond locations/geometries as well as in the position of the acyl chain with resolving power (R) up to ~410 (R~320 needed on average). Extremely small structural differences exhibiting collision cross sections (CCS) of less than 1% (down to 0.2%) are sufficient for the discrimination of the isomeric lipid species using TIMS-MS. The same level of performance was maintained in the complex biological mixture for the biologically relevant PC 16:0/18:1 lipid isomers. These results suggest several advantages of using complementary LC-TIMS-MS separations for regular lipidomic analysis, with main emphasis in the elucidation of isomer-specific lipid biological activities.

Lipids are essential small-molecule metabolites that play many important roles in a wide variety of physiological processes.[1, 2] The lipid composition of different membranes substantially varies throughout the cell,[3, 4] suggesting that different lipids are required depending on the needed function.[5] Dysregulation of lipid metabolism has been associated with various pathologies,[6] including atherosclerosis,[7] infections,[8] cancers,[9, 10] diabetes[11] and neurodegenerative diseases.[12] Understanding the biological roles and mechanisms of lipids is still full of challenges because of their variation in headgroups and aliphatic chains that may exist in any eukaryotic cell.[13] In fact, the complexity and diversity of lipid structures and functions approach those of proteins.[14] Despite their clear importance and essential functions, lipids have been significantly less studied when compare to proteins. In addition, the number, abundance, and biomedical importance of lipids may be profoundly underestimated due to challenges with current analytical separation techniques. Thus, the development of new analytical tools able to discriminate isomeric lipid species is essential for investigating their physiological roles in health and disease.

The study of lipids in biological systems has fundamentally advanced the understanding of the lipidomic area in recent years.[2, 15-18] Although nuclear magnetic resonance (NMR)[19, 20] and X-ray diffraction[21, 22] can be used to identify and characterize bulk lipid properties, advances in lipidomics are substantially driven by mass spectrometry (MS), mainly using shotgun lipidomics,[23-25] and liquid chromatography (LC) coupled to MS.[26-30] Lipids are generally detected over a relatively narrow mass-to-charge (m/z) range (m/z 500-1200) leading to a large number of lipid species having the same nominal mass (i.e. isomers and isobars) which makes their identification and characterization challenging. LC-MS approaches have shown potential for the identification and separation of isomeric lipid species, but those separations require relatively long analysis times and are not universal for all lipid classes.[31] Tandem mass spectrometry (MS/MS) using different modes of activation (e.g., collision induced dissociation (CID),[32-34] Paterno–Buchi (P–B) reaction followed by CID,[35, 36] ozone

induced dissociation (OzID),[37-39] electron induced dissociation (EID),[40, 41] radical directed dissociation (RDD)[42] and photodissociation,[43, 44]) has demonstrated significant advances in elucidating isomeric lipid species, such as double bond position (P-B, OzID and EID) and positional isomers (*sn*-1 and *sn*-2) (MS^3 with CID). However, these technique have struggled to quantify isomers due to differences in dissociation efficiencies between isomers and separation techniques to complement ion activation are needed to provide the unequivocal structural assignment.

Ion mobility spectrometry (IMS) coupled to MS has promise in lipid isomer separation, especially when combined with liquid chromatography. While LC separation is often on the order of minutes, a second dimension of separation based on mobility (or size/charge) can be performed in a millisecond timescale, leading to higher selectivity, reduced chemical noise and increased peak capacity.[45-47] Lipidomic studies can be performed using the five major IMS separation techniques available: drift tube IMS (DTIMS),[48, 49] traveling wave IMS (TWIMS),[49, 50] field asymmetric IMS (FAIMS),[51] structures for lossless ion manipulations (SLIM)[49, 52, 53] and trapped IMS (TIMS).[49, 54, 55] IMS techniques can be coupled with LC in order to provide an additional dimension of separation that further increase peak capacity and specificity for lipid identification.[56-58] The use of IMS–MS in shotgun lipidomics has previously demonstrated utility using DTIMS,[59-61] TWIMS[62-64] and FAIMS,[65, 66] for the separation of isomeric lipid species from distinct categories and subclasses improving lipid fingerprinting and identification. However, in some case, the IMS resolving power has been limited resulting in unresolved isomeric lipid species in complex biological mixtures.[67] Recent studies using high resolution FAIMS[68] and the SLIM technology[69] showed great promise for the identification and separation of isomeric lipid species presenting subtle structural differences. Although these approaches are powerful by providing ultra-high resolving power, the use of the high resolution FAIMS and SLIM technologies is not yet widely available. The recent introduction of TIMS and its integration with MS analyzers has showed its potential for separation and structural elucidation of biomolecules by providing high resolving power (R up to 400 in 50-500 ms).[70-76] In a recent study, the analytical power of LC-TIMS-MS has been demonstrated for non-targeted analysis of human plasma, where a great number of compounds with equal retention times but separated in the TIMS dimension and vice-versa, showing the good orthogonality and analytical potential of combining LC and TIMS for the identification and separation of the major lipid classes.[77] Since the introduction of a commercial TIMS-MS instrument in 2016, providing high mobility resolution in a q-TOF MS/MS platform, the interest in potential integration of high resolution linear IMS to traditional LC-MS/MS workflows has increased significantly.

In the present work, a combination of LC followed by high resolution TIMS-MS was used to investigate selected isomeric glycerophosphocholine (PC) and diacylglycerol (DG) standard lipid species which differ from their lipid acyl chain positions and/or double bond locations and geometries (Figure 1). The present workflow was also evaluated for the separation and identification of the biologically relevant PC 16:0/18:1 lipid isomers from human plasma. Different from previous work, a special emphasis is placed on the capability of high resolution linear IMS in LC compatible time scales (e.g., TIMS in 50-500 ms) for the separation of isomeric lipid species with extremely small structural differences.

EXPERIMENTAL SECTION

Materials and Reagents

The present study involves 14 lipids including 6 glycerophosphocholine (PC) and 8 diacylglycerol (DG) illustrated in Figure 1. The isomeric lipid standards were selected according to their lipid acyl chain positions and double bond locations and geometries. All the investigated PC and DG lipids were purchased from Avanti Polar Lipids (Alabaster, AL) and Nu-Chek Prep (Elysian, MN), respectively. Lipid solutions were prepared at a final concentration of 5 µM in 5:95 water/methanol (H_2O/MeOH). Human plasma (SRM 1950) was purchased from the National Institute of Standards and Technology (NIST; Gaithersburg, MD). The lipid extraction from human plasma was performed as described elsewhere.[78] Calibration standard (Tuning Mix, G1969-85000) was purchased from Agilent Technologies (Santa Clara, CA) and used to calibrate the instruments.

LC-TIMS-MS Experiments

Liquid chromatography was performed by a Prominence LC-20AD HPLC system (Shimadzu, Japan), equipped with an Acclaim 120 C18 Column, 50 × 3.0 mm × 3 µm (Thermo Scientific, USA) which was kept at 55° C. Gradient separations were performed between 60:40 H_2O/ACN and 89:10:1 IPA/ACN/H_2O, both containing 10 mM ammonium formate and 0.1 % formic acid. Flow rate was varied (0.60-0.75 mL/min) and total run time was 25 min (details in Table S1).

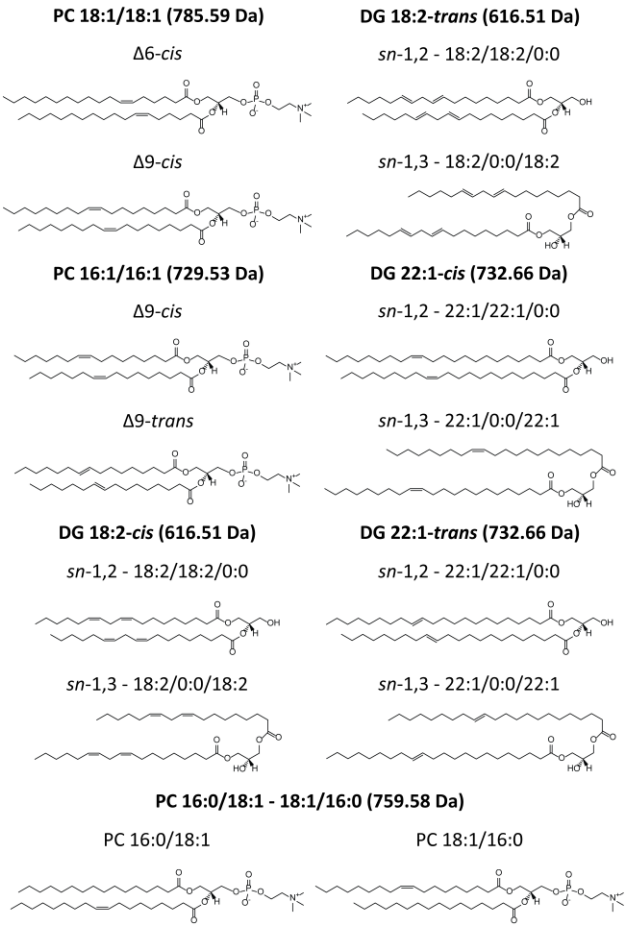

Figure 1. Overview of the investigated glycerophosphocholine (PC) and diacylglycerol (DG) standard lipid structures.

Briefly, the ion mobility separation in a TIMS device is based on holding the ions stationary using an electric field (E) against a moving buffer gas (Figure S1).[54, 55] In TIMS operation, multiple isomers are trapped simultaneously at different E values resulting from a voltage gradient applied across the IMS tunnel region (Figure S1). After thermalization, isomers are eluted by decreasing the electric field in stepwise decrements (Figure S1). TIMS separation depends on the gas flow velocity (v_g), elution voltage ($V_{elution}$), ramp time (t_{ramp}) and base voltage (V_{out}).[54] The reduced mobility, K_o, is defined by:

$$K_0 = \frac{v_g}{E} \cong \frac{A}{(V_{elution} - V_{out})} \quad (1)$$

The constant A is determined using calibration standards (Tuning Mix) of known reduced mobilities,[79] as previously reported for the case of lipids.[77] The measured mobilities are converted into collision cross sections (CCS, Ω in Å²) using the Mason-Schamp equation:

$$\Omega = \frac{(18\pi)^{1/2}}{16} \frac{q}{(k_B T)^{1/2}} \left(\frac{1}{m} + \frac{1}{M}\right)^{1/2} \frac{1}{N} \times \frac{1}{K} \quad (2)$$

where q is the ion charge, k_B is the Boltzmann constant, N is the gas number density, m is the ion mass, and M is the gas molecule mass.[80]

LC-TIMS-MS detection was performed using a Bruker timsTOF instrument, equipped with an ESI source operated in positive mode at capillary and end plate voltages fixed at 4500 V and 500 V, respectively, under nitrogen flow at 8.0 L/min and 200 °C. In the case of LC-TIMS-MS, internal mass and ion mobility calibrations were performed by post-column introduction of calibration standards at the beginning and at the end of each run. LC-TIMS-MS mobility calibration was performed using a linear fit between the scan number and the $1/K_o$ of known reduced mobilities. Complementary nESI-TIMS-MS experiments were performed on binary mixtures using a custom built TIMS device coupled to a Bruker Maxis Impact II q-TOF MS, and mobility calibration was performed as described previously.[79] The buffer gas was nitrogen (N_2) at room temperature (T), and velocity of the bath gas was defined by the pressure difference between the entrance (P1=2.6 mbar) and exit (P2=1.1 mbar) of the TIMS analyser. An rf voltage of 250 V_{pp} at 880 kHz was applied to all electrodes. The scan rate ($Sr = \Delta V_{ramp}/t_{ramp}$), was optimized for the binary mixtures, due to the different degree of complexity (Table S2). In practice, Sr is reduced by decreasing V_{ramp}, and/or increasing t_{ramp}. Note that as t_{ramp} increases, lower ion signal intensity may be observed due to distribution of the ion mobility band over a larger number of channels (almost same area). For TIMS, the resolving power R and resolution r of the IMS bands are defined as $R = \Omega/w$ and $r = 1.18*(\Omega_2-\Omega_1)/(w_1+w_2)$, where w is the full peak width at half maximum (FWHM). Same metrics for the LC peaks were computed with Ω replaced by t_R.

RESULTS AND DISCUSSION

A large component within the isomeric lipid diversity comes from positional isomers based on the acyl chains locations along the lipid backbone (*sn*-1, *sn*-2, or *sn*-3) and/or the different locations of double bonds and geometries (*cis* or *trans*). LC-TIMS experiments were acquired as individual lipid isomers and as mixtures. The measured collision cross sections (CCS) and resolving power (R), resolution (r) and scan rate (Sr) metrics are listed in Tables S2 and S3. The calculated CCS values were found consistent with previous reported CCS (within ~1%) using different IMS technologies as well as calibration standards.[61, 64]

LC-TIMS Separation of Lipid Isomers with Varying Double Bond Locations and Geometries

The present workflow was initially assessed by exploring structurally similar PC lipid isomers comprising different double bond locations with the same geometry (Figure 2a) and different double bond orientations at the same position (Figure 2b). The LC dimension was very effective by providing a baseline separation for the PC 18:1/18:1 Δ6-Δ9-*cis* (r ~ 1.5, Figure 2a) and PC 16:1/16:1 Δ9-*cis*/*trans* (r ~ 1.9, Figure 2b) lipid isomers. The apparent R of ~ 85 - 135 in the mobility dimension only allowed partial (if any) PC lipid separation using fast scan rates [Sr = 0.3 V/ms] for the protonated and sodiated species (Figure 2). In fact, similar features in the mobility spectra are observed for the protonated (r ~ 0.25) and sodiated (r ~ 0.05) species of PC 16:1/16:1 Δ9-*cis*/*trans*, and slightly different features for the protonated (r ~ 0.5) and sodiated (r ~ 0.6) species of PC 18:1/18:1 Δ6-Δ9-*cis*. Slower scan rates [Sr = 0.012 – 0.02 V/ms] experiments were performed on these PC lipid isomers leading to a significant increase of the mobility resolving power (R ~ 230 – 385). The slower scan rates deliver a baseline separation for the protonated (r ~ 1.4) and sodiated (r ~ 1.5) species of PC 18:1/18:1 Δ6-Δ9-*cis* (Figure 2a) while the protonated species of PC 16:1/16:1 Δ9-*cis*/*trans* are separated in their mixture (r ~ 0.8, Figure 2b). Concerning the sodiated species of PC 16:1/16:1 Δ9-*cis*/*trans*, the two lipid isomers coincided (r ~ 0.2) even at R ~ 230 reached at slow scan rates (Figure 2b). This suggests that the interaction of the sodium metal ion with the fatty acyl chain of PC 16:1/16:1 Δ9-*trans* leads to a folding of the *trans*-fatty acyl chain adopting a closed structure as compared to the sodiated species of PC 16:1/16:1 Δ9-*cis*. In addition to the high resolving power provided by the TIMS analyzer, accurate measurement of their relative ($\Delta\Omega_r$) and absolute ($\Delta\Omega$) mobility differences with 0.35% (1.0 Å²) for the protonated species of PC 16:1/16:1 Δ9-*cis*/*trans* and 0.89% (2.7 Å²) and 0.91% (2.8 Å²) for the protonated and sodiated species of PC 18:1/18:1 Δ6-Δ9-*cis* are reported, respectively (Table S3).

Comparison of the TIMS performance on PC 18:1/18:1 Δ6-Δ9-*cis* with other IMS technologies shows similar separation trends as obtained in SLIM[69] and AP-DTIMS[61] but better than reported with high resolution FAIMS,[68] for which the lipid isomers are not separated. For PC 16:1/16:1 Δ9-*cis*/*trans*, the TIMS separation exhibits better performance than the separation obtained in AP-DTIMS[61] and similar to that of the SLIM 15.9 m path length.[69] Moreover, high resolution FAIMS baseline resolves these two lipid isomers in mixture.[68] These two examples evidence the orthogonality between FAIMS and linear IMS technologies (e.g., DTIMS[81] and TIMS[82]) for the case of lipids. Hence, the TIMS technology appears to be sufficiently powerful when compared to the other IMS technologies and has the advantage of being commercially available.

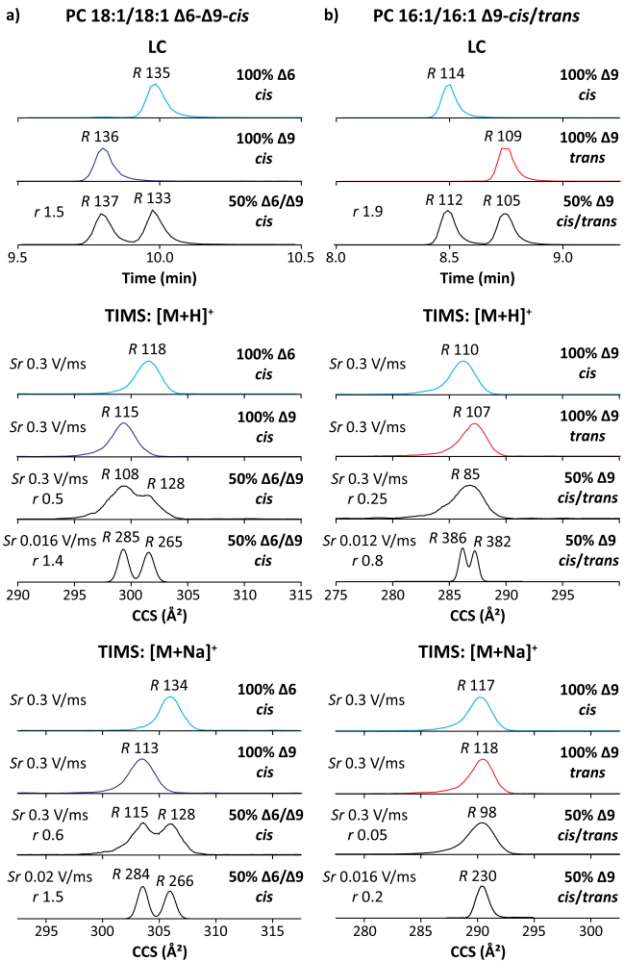

Figure 2. Typical LC and TIMS spectra for the protonated and sodiated species of (a) PC 18:1/18:1 Δ6-Δ9-*cis* and (b) PC 16:1/16:1 Δ9-*cis*/*trans*. The isomeric species are colored in blue (*cis*) and red (*trans*). The TIMS spectra for mixtures (black) employed different scan rates (Sr) as marked. The R and r values are given.

Moreover, the protonated species of PC 16:1/16:1 Δ9-*cis* showed more compact structures than PC 16:1/16:1 Δ9-*trans* (Figure 2b). Concerning PC 18:1/18:1 Δ6-Δ9-*cis*, the protonated and sodiated species of PC 18:1/18:1 Δ6-*cis* exhibited more extended structures than PC 18:1/18:1 Δ9-*cis* (Figure 2a). These TIMS results are consistent with the elution order reported for other IMS technologies.[47] While the LC and TIMS (when using slow scan rates) separations were comparable (r ~ 1.5 and r ~ 1.9 vs r ~ 1.5 and r ~ 0.8, respectively) during the separation of lipid isomers comprising distinct double bond locations and geometries, the shorter time scale of the TIMS separation allows for easy integration in a LC-TIMS-MS workflow.

LC-TIMS Separation of Lipid Isomers with Varying Acyl Chain Positions and Double Bond Geometries

The present workflow was assessed with DG lipid isomers comprising different acyl chain positions and double bond geometries (Figures 3 and S2). The LC dimension was very effective by providing nearly baseline separation for the DG *sn*-1,2 22:1-*cis*/*trans* (r ~ 0.9) and DG *sn*-1,3 22:1-*cis*/*trans* (r ~ 1.1, Figure 3a) and a baseline separation for the DG *sn*-1,2 18:2-*cis*/*trans* (r ~ 2.0) and DG *sn*-1,3 18:2-*cis*/*trans* (r ~ 2.2, Figure S2a) lipid isomers. However, the LC dimension was not able to separate DG lipid isomers with different acyl chain positions but with the same double bond geometries. The sodiated species of DG *sn*-1,2/*sn*-1,3 22:1-*cis*/*cis*, DG *sn*-1,2/*sn*-1,3 22:1-*trans*/*trans*, DG *sn*-1,2/*sn*-1,3 18:2-*cis*/*cis* and DG *sn*-1,2/*sn*-1,3 18:2-*trans*/*trans* were investigated in the mobility dimension. No separation (r < 0.2) was obtained in the TIMS dimension using fast scan rates [Sr = 0.3 V/ms, R ~ 55 - 100] for any of the sodiated species of DG lipid isomers (Figures 3bc and S2bc). Slower scan rates [Sr = 0.016 – 0.02 V/ms] experiments were performed on these DG lipid isomers resulting in an increase of the separation due to significant increase of their resolving power values (R ~ 230 – 405). Although the DG lipid isomers were not baseline resolved, the sodiated species of DG *sn*-1,2/*sn*-1,3 22:1-*cis*/*cis* (r ~ 0.65), DG *sn*-1,2/*sn*-1,3 22:1-*trans*/*trans* (r ~ 0.65) and DG *sn*-1,2/*sn*-1,3 18:2-trans/trans (r ~ 0.75) can be separated in a mixture (Figures 3bc and S2bc). These partial separation, with R ~ 350 in average, are related to the extremely small structural differences of the sodiated species of DG *sn*-1,2/*sn*-1,3 22:1-*cis*/*cis* (0.23%, 0.7 Å²), DG *sn*-1,2/*sn*-1,3 22:1-trans/trans (0.30%, 0.9 Å²) and DG *sn*-1,2/*sn*-1,3 18:2-trans/trans (0.32%, 0.8 Å², Table S3).

In addition, the structural differences between the isomeric DG lipid species comprising the same acyl chain positions but different double bond geometries were larger when comparing their CCS profiles and even more pronounced when multiple double bonds are present and therefore better separated (Figures 3de and S2de). For example, mobility differences of 0.42% (1.2 Å²), 0.56% (1.5 Å²) and 0.79% (2.1 Å²) were observed for DG *sn*-1,3 22:1-*cis*/*trans*, DG *sn*-1,2 18:2-*cis*/*trans* and DG *sn*-1,3 18:2-*cis*/*trans*, respectively (Table S3). This delivers nearly baseline separations for DG *sn*-1,2 18:2-*cis*/*trans* (r ~ 1.15) and DG *sn*-1,3 18:2-*cis*/*trans* (r ~ 1.25) and separate DG *sn*-1,3 22:1-*cis*/*trans* (r ~ 0.75). The analysis of *sn*-1/*sn*-2 or *sn*-3 separations with similar acyl chains and double bond geometries suggests that more compact structures are observed when the acyl chains are in position *sn*-1,2 as compared to positions *sn*-1,3. The DG lipid isomers with

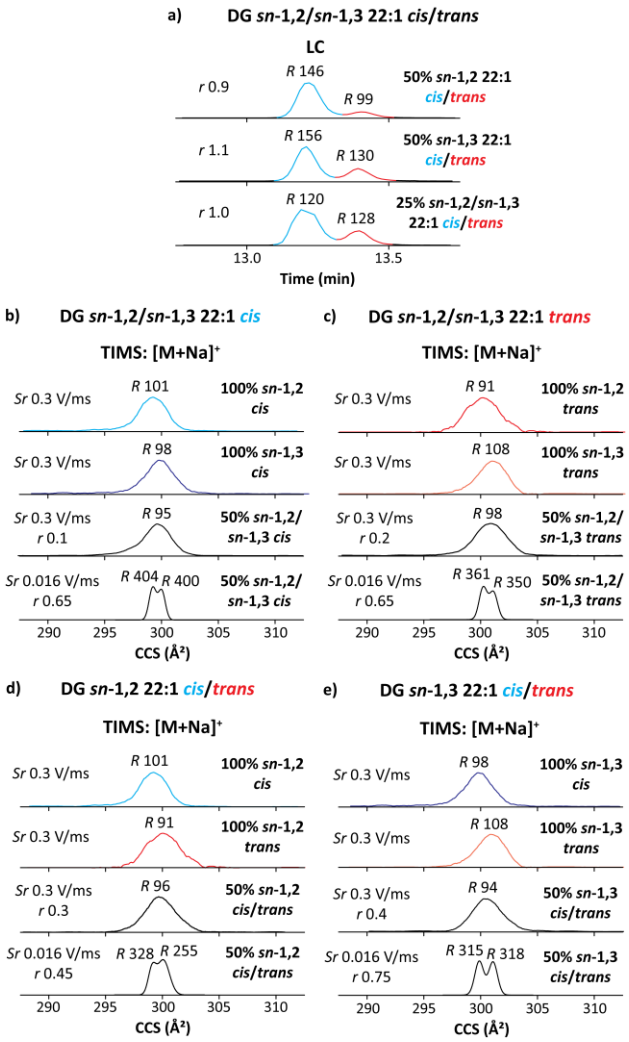

Figure 3. Typical LC (a) and TIMS (b-e) spectra for the sodiated species of DG *sn*-1,2/*sn*-1,3 22:1-*cis*/*trans*. The isomeric species are colored in blue (*cis*) and red (*trans*). The TIMS spectra for mixtures (black) employed different scan rates (Sr) as marked. The R and r values are given.

similar acyl chain positions and *cis* double bonds have more compact structures than those with *trans* double bonds. In addition, this trend is more pronounced when multiple double bonds are present in the DG lipid isomers. These examples clearly evidence the orthogonality between the LC and TIMS dimensions, where separation of lipid isomers comprising distinct acyl chain positions (*sn*-1,2/*sn*-1,3) and double bond geometries (*cis*/*trans*) is more powerful in the LC dimension while separation of lipid isomers with distinct acyl chain positions but same double bond geometries is more effective in the TIMS dimension.

The present workflow was finally evaluated in a human plasma complex mixture. As shown in Figure 4a, LC-TIMS-MS heat map identified different classes of lipids including lysophosphatidylcholine (LPC), diacylglycerol (DG), phosphatidylethanolamine (PE), phosphatidylcholine (PC), sphingomyelin (SM), triacylglycerol (TG) and cholesteryl ester (CE). The tentative assignment of individual lipid classes was based on a previous study using LC-TIMS-MS.[77] This clearly demonstrates a highly informative structural identification of the biological complex mixture with a great number of compounds with equal retention times but separated in the TIMS dimension. This statement was verified for the case of the biologically relevant PC 16:0/18:1 lipid isomers comprising different acyl chain positions (*sn*-1/*sn*-2) with the same double bond geometries (*cis*, Figure 4b). The LC dimension was not able to separate the PC 16:0/18:1 lipid isomers. The protonated species of the PC 16:0/18:1 (purple traces) and PC 18:1/16:0 (green traces) standards lipid isomers were investigated in the TIMS dimension. No separation (r ~ 0.2) was obtained using fast scan rates [Sr = 0.3 V/ms, R ~ 120] for the two isomeric lipid species in the biological sample (Figure 4b, black traces). Slower scan rates [Sr = 0.016 V/ms, R ~ 400] experiments permitted to identify (r ~ 0.6) the two lipid isomers in the human plasma complex mixture, with PC 16:0/18:1 and PC 18:1/16:0 accounting for 86% and 14%, respectively (Figure 4b, color traces). This ratio was consistent with previous work performed with CID (MS^3)[83] and AP-DTIMS.[61] The partial separation is related to the extremely small structural differences of the protonated species of PC 16:0/18:1 and PC 18:1/16:0 (0.22%, 0.7 Å^2, Table S3).

Comparison between the present TIMS data and reported AP-DTIMS data[61] shows better performance for the TIMS on the biologically relevant PC 16:0/18:1 lipid isomers, as AP-DTIMS uses silver adduction to separate these lipid isomers. However, high resolution FAIMS experiments[68] exhibited better separation than TIMS also giving promise for the FAIMS/TIMS-MS integration for lipidomic studies. As previously shown,[67] the smaller acyl chains in the *sn*-1 position give the more compact lipid structures, as reflected by the slightly lower CCS value for the protonated species of PC 16:0/18:1 when compared to PC 18:1/16:0 (Figure 4b and Table S3). This example provides clear evidence of the orthogonality between the LC and TIMS dimensions as well as the advantages of the LC-TIMS integration for biological mixture, since the lipid species are not separated in the LC dimension using common LC separations.

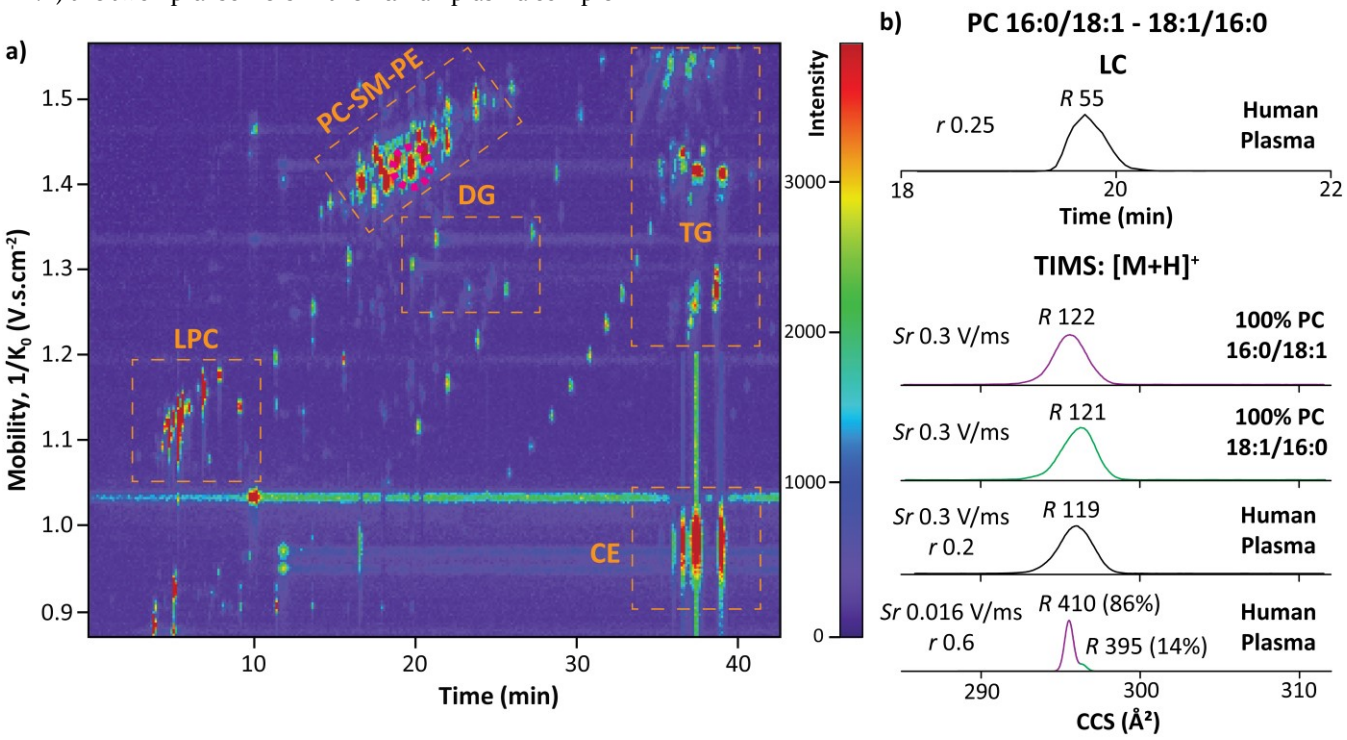

Figure 4. (a) LC-TIMS–MS heat map of human plasma complex mixture. Tentative regions (orange dashed) are assigned to different classes of lipids. (b) Typical LC and TIMS spectra for the protonated species of PC 16:0/18:1 – 18:1/16:0. The isomeric species are colored in purple (16:0/18:1) and green (18:1/16:0). The TIMS spectra for mixtures (black) employed different scan rates (Sr) as marked. The R and r values are given.

CONCLUSIONS

The potential of LC-TIMS-MS with high mobility resolving power (R up to ~410) is described for the case of PC and DG standard lipids isomers as well from human plasma, with extremely small structural differences ($\Delta\Omega$ down to ~0.2%, 0.6 Å^2). In one hand, the LC dimension was effective for the separation of lipid isomers comprising distinct double bond locations and/or geometries, but was limited during the separation of lipid isomers with distinct acyl chain positions. On the other hand, the TIMS dimension resulted in the identification of almost all the investigated lipid isomers, and was consistent with reported IMS data using other IMS variants. The same level of performance was maintained in the complex biological mixture for the biologically relevant PC 16:0/18:1 lipid isomers Comparison of the TIMS performance with DTIMS technologies shows better separation with TIMS as compared to low pressure DTIMS and atmospheric pressure DTIMS (AP-DTIMS). Moreover, the TIMS technology exhibited comparable performance to the SLIM 15.9 m path length technology. The orthogonality between the LC and TIMS dimension combined with the performance metrics of the LC-TIMS-MS integration for biological mixture suggest great promise for lipidomic studies. Many of the investigated lipid isomers showcase the analytical challenge for mobility technologies during lipidomic studies (e.g., extremely small structural differences). The high resolution FAIMS was shown to be orthogonal to linear IMS (e.g., TIMS) during the separation of lipid species, suggesting great potential for complementary non-linear and linear IMS (i.e., FAIMS-TIMS-MS) to advance global lipid analysis in complex biological systems.

ASSOCIATED CONTENT

Supporting Information

TIMS-MS instrument showing the TIMS cell schematic and TIMS operation, additional LC and TIMS spectra of the investigated lipid isomers and Tables of the measured separation parameters, resolution metrics and scan rates for all isomeric lipid species. This material is available free of charge via the Internet at http://pubs.acs.org.

AUTHOR INFORMATION

Corresponding Author

fernandf@fiu.edu

Notes

The authors declare no competing financial interest.

ACKNOWLEDGEMENTS

The authors acknowledge the financial support from the National Institute of Allergy and Infectious Diseases award R21AI135469 and the National Science Foundation Division of Chemistry, under CAREER award CHE-1654274, with co-funding from the Division of Molecular and Cellular Biosciences to F.F.-L. The authors wish to acknowledge Dr. Mark E. Ridgeway and Dr. Melvin A. Park from Bruker Daltonics, Inc. during the development and implementation of TIMS-MS experiments.

REFERENCES

1. Yeagle, P. L., Lipid regulation of cell membrane structure and function. *FASEB J.* **1989,** *3* (7), 1833-1842.
2. Wenk, M. R., The emerging field of lipidomics. *Nat. Rev. Drug Discov.* **2005,** *4* (7), 594-610.
3. van Meer, G.; Voelker, D. R.; Feigenson, G. W., Membrane lipids: where they are and how they behave. *Nat. Rev. Mol. Cell Biol.* **2008,** *9* (2), 112-124.
4. Jackson, C. L.; Walch, L.; Verbavatz, J. M., Lipids and Their Trafficking: An Integral Part of Cellular Organization. *Develop. Cell* **2016,** *39* (2), 139-153.
5. Klose, C.; Surma, M. A.; Simons, K., Organellar lipidomics--background and perspectives. *Curr. Opin. Cell Biol.* **2013,** *25* (4), 406-413.
6. Wymann, M. P.; Schneiter, R., Lipid signalling in disease. *Nat. Rev. Mol. Cell Biol.* **2008,** *9* (2), 162-176.
7. Berliner, J. A.; Leitinger, N.; Tsimikas, S., The role of oxidized phospholipids in atherosclerosis. *J. Lipid Res.* **2009,** *50 Suppl*, S207-212.
8. Marsh, M.; Helenius, A., Virus entry: open sesame. *Cell* **2006,** *124* (4), 729-740.
9. Santos, C. R.; Schulze, A., Lipid metabolism in cancer. *FEBS J.* **2012,** *279* (15), 2610-2623.
10. Sounni, N. E.; Cimino, J.; Blacher, S.; Primac, I.; Truong, A.; Mazzucchelli, G.; Paye, A.; Calligaris, D.; Debois, D.; De Tullio, P.; Mari, B.; De Pauw, E.; Noel, A., Blocking lipid synthesis overcomes tumor regrowth and metastasis after antiangiogenic therapy withdrawal. *Cell Metab.* **2014,** *20* (2), 280-294.
11. Gross, R. W.; Han, X., Lipidomics in diabetes and the metabolic syndrome. *Methods Enzymol.* **2007,** *433*, 73-90.
12. Sagin, F.; Sozmen, E., Lipids as Key Players in Alzheimer Disease - Alterations in Metabolism and Genetics. *Curr. Alzheimer Res.* **2008,** *5* (1), 4-14.
13. Sud, M.; Fahy, E.; Cotter, D.; Brown, A.; Dennis, E. A.; Glass, C. K.; Merrill, A. H., Jr.; Murphy, R. C.; Raetz, C. R.; Russell, D. W.; Subramaniam, S., LMSD: LIPID MAPS structure database. *Nucleic Acids Res.* **2007,** *35* (Database issue), D527-532.
14. Muro, E.; Atilla-Gokcumen, G. E.; Eggert, U. S., Lipids in cell biology: how can we understand them better? *Mol. Biol. Cell* **2014,** *25* (12), 1819-1823.
15. Quehenberger, O.; Armando, A. M.; Brown, A. H.; Milne, S. B.; Myers, D. S.; Merrill, A. H.; Bandyopadhyay, S.; Jones, K. N.; Kelly, S.; Shaner, R. L.; Sullards, C. M.; Wang, E.; Murphy, R. C.; Barkley, R. M.; Leiker, T. J.; Raetz, C. R.; Guan, Z.; Laird, G. M.; Six, D. A.; Russell, D. W.; McDonald, J. G.; Subramaniam, S.; Fahy, E.; Dennis, E. A., Lipidomics reveals a remarkable diversity of lipids in human plasma. *J. Lipid Res.* **2010,** *51* (11), 3299-3305.

16. Dennis, E. A.; Deems, R. A.; Harkewicz, R.; Quehenberger, O.; Brown, H. A.; Milne, S. B.; Myers, D. S.; Glass, C. K.; Hardiman, G.; Reichart, D.; Merrill, A. H., Jr.; Sullards, M. C.; Wang, E.; Murphy, R. C.; Raetz, C. R.; Garrett, T. A.; Guan, Z.; Ryan, A. C.; Russell, D. W.; McDonald, J. G.; Thompson, B. M.; Shaw, W. A.; Sud, M.; Zhao, Y.; Gupta, S.; Maurya, M. R.; Fahy, E.; Subramaniam, S., A mouse macrophage lipidome. *J. Biol. Chem.* **2010,** *285* (51), 39976-39985.

17. Brown, H. A.; Murphy, R. C., Working towards an exegesis for lipids in biology. *Nat. Chem. Biol.* **2009,** *5* (9), 602-606.

18. Shevchenko, A.; Simons, K., Lipidomics: coming to grips with lipid diversity. *Nat. Rev. Mol. Cell Biol.* **2010,** *11* (8), 593-598.

19. Gunstone, F. D.; Shukla, V. K. S., NMR of Lipids. *Annu. Rep. NMR Spectrosc.* **1995,** *31*, 219-237.

20. Pikula, S.; Bandorowicz-Pikula, J.; Groves, P., Recent Advances in NMR Studies of Lipids. *Annu. Rep. NMR Spectrosc.* **2015,** *85*, 195-246.

21. Ziblat, R.; Leiserowitz, L.; Addadi, L., Crystalline lipid domains: characterization by X-ray diffraction and their relation to biology. *Angew. Chem.* **2011,** *50* (16), 3620-3629.

22. Tyler, A. I.; Law, R. V.; Seddon, J. M., X-ray diffraction of lipid model membranes. *Methods Mol. Biol.* **2015,** *1232*, 199-225.

23. Han, X.; Gross, R. W., Shotgun lipidomics: electrospray ionization mass spectrometric analysis and quantitation of cellular lipidomes directly from crude extracts of biological samples. *Mass Spectrom. Rev.* **2005,** *24* (3), 367-412.

24. Schwudke, D.; Liebisch, G.; Herzog, R.; Schmitz, G.; Shevchenko, A., Shotgun lipidomics by tandem mass spectrometry under data-dependent acquisition control. *Methods Enzymol.* **2007,** *433*, 175-191.

25. Graessler, J.; Schwudke, D.; Schwarz, P. E.; Herzog, R.; Shevchenko, A.; Bornstein, S. R., Top-down lipidomics reveals ether lipid deficiency in blood plasma of hypertensive patients. *PloS One* **2009,** *4* (7), e6261.

26. Knittelfelder, O. L.; Weberhofer, B. P.; Eichmann, T. O.; Kohlwein, S. D.; Rechberger, G. N., A versatile ultra-high performance LC-MS method for lipid profiling. *J. Chromatogr. B.* **2014,** *951-952*, 119-128.

27. Sommer, U.; Herscovitz, H.; Welty, F. K.; Costello, C. E., LC-MS-based method for the qualitative and quantitative analysis of complex lipid mixtures. *J. Lipid Res.* **2006,** *47* (4), 804-814.

28. Fauland, A.; Kofeler, H.; Trotzmuller, M.; Knopf, A.; Hartler, J.; Eberl, A.; Chitraju, C.; Lankmayr, E.; Spener, F., A comprehensive method for lipid profiling by liquid chromatography-ion cyclotron resonance mass spectrometry. *J. Lipid Res.* **2011,** *52* (12), 2314-2322.

29. Cajka, T.; Fiehn, O., Comprehensive analysis of lipids in biological systems by liquid chromatography-mass spectrometry. *Trends Anal. Chem.* **2014,** *61*, 192-206.

30. Sokol, E.; Almeida, R.; Hannibal-Bach, H. K.; Kotowska, D.; Vogt, J.; Baumgart, J.; Kristiansen, K.; Nitsch, R.; Knudsen, J.; Ejsing, C. S., Profiling of lipid species by normal-phase liquid chromatography, nanoelectrospray ionization, and ion trap-orbitrap mass spectrometry. *Anal. Biochem.* **2013,** *443* (1), 88-96.

31. Sandra, K.; Sandra, P., Lipidomics from an analytical perspective. *Curr. Opin. Chem. Biol.* **2013,** *17* (5), 847-853.

32. Esch, S. W.; Tamura, P.; Sparks, A. A.; Roth, M. R.; Devaiah, S. P.; Heinz, E.; Wang, X.; Williams, T. D.; Welti, R., Rapid characterization of the fatty acyl composition of complex lipids by collision-induced dissociation time-of-flight mass spectrometry. *J. Lipid Res.* **2007,** *48* (1), 235-241.

33. Chan, S.; Reinhold, V. N., Detailed structural characterization of lipid A: electrospray ionization coupled with tandem mass spectrometry. *Anal. Biochem.* **1994,** *218* (1), 63-73.

34. Hale, O. J.; Cramer, R., Collision-induced dissociation of doubly-charged barium-cationized lipids generated from liquid samples by atmospheric pressure matrix-assisted laser desorption/ionization provides structurally diagnostic product ions. *Anal. Bioanal. Chem.* **2018,** *410* (5), 1435-1444.

35. Ma, X.; Xia, Y., Pinpointing double bonds in lipids by Paterno-Buchi reactions and mass spectrometry. *Angew. Chem.* **2014,** *53* (10), 2592-2596.

36. Ma, X.; Zhao, X.; Li, J.; Zhang, W.; Cheng, J. X.; Ouyang, Z.; Xia, Y., Photochemical Tagging for Quantitation of Unsaturated Fatty Acids by Mass Spectrometry. *Anal. Chem.* **2016,** *88* (18), 8931-8935.

37. Thomas, M. C.; Mitchell, T. W.; Harman, D. G.; Deeley, J. M.; Nealon, J. R.; Blanksby, S. J., Ozone-induced dissociation: elucidation of double bond position within mass-selected lipid ions. *Anal. Chem.* **2008,** *80* (1), 303-311.

38. Brown, S. H.; Mitchell, T. W.; Blanksby, S. J., Analysis of unsaturated lipids by ozone-induced dissociation. *Biochim. Biophys. Acta* **2011,** *1811* (11), 807-817.

39. Poad, B. L.; Green, M. R.; Kirk, J. M.; Tomczyk, N.; Mitchell, T. W.; Blanksby, S. J., High-Pressure Ozone-Induced Dissociation for Lipid Structure Elucidation on Fast Chromatographic Timescales. *Anal. Chem.* **2017,** *89* (7), 4223-4229.

40. Yoo, H. J.; Hakansson, K., Determination of double bond location in fatty acids by manganese adduction and electron induced dissociation. *Anal. Chem.* **2010,** *82* (16), 6940-6946.

41. Jones, J. W.; Thompson, C. J.; Carter, C. L.; Kane, M. A., Electron-induced dissociation (EID) for structure characterization of glycerophosphatidylcholine: determination of double-bond positions and localization of acyl chains. *J. Mass Spectrom.* **2015,** *50* (12), 1327-1339.

42. Pham, H. T.; Ly, T.; Trevitt, A. J.; Mitchell, T. W.; Blanksby, S. J., Differentiation of complex lipid isomers by radical-directed dissociation mass spectrometry. *Anal. Chem.* **2012,** *84* (17), 7525-7532.

43. Madsen, J. A.; Cullen, T. W.; Trent, M. S.; Brodbelt, J. S., IR and UV photodissociation as analytical tools for characterizing lipid A structures. *Anal. Chem.* **2011,** *83* (13), 5107-5113.

44. O'Brien, J. P.; Needham, B. D.; Henderson, J. C.; Nowicki, E. M.; Trent, M. S.; Brodbelt, J. S., 193 nm ultraviolet photodissociation mass spectrometry for the structural elucidation of lipid A compounds in complex mixtures. *Anal. Chem.* **2014,** *86* (4), 2138-2145.

45. Kliman, M.; May, J. C.; McLean, J. A., Lipid analysis and lipidomics by structurally selective ion mobility-mass spectrometry. *Biochim. Biophys. Acta* **2011,** *1811* (11), 935-945.

46. Paglia, G.; Kliman, M.; Claude, E.; Geromanos, S.; Astarita, G., Applications of ion-mobility mass spectrometry for lipid analysis. *Anal. Bioanal. Chem.* **2015,** *407* (17), 4995-5007.

47. Zheng, X.; Smith, R. D.; Baker, E. S., Recent advances in lipid separations and structural elucidation using mass spectrometry combined with ion mobility spectrometry, ion-molecule reactions and fragmentation approaches. *Curr. Opin. Chem. Biol.* **2018,** *42*, 111-118.

48. Revercomb, H. E.; Mason, E. A., Theory of plasma chromatography/gaseous electrophoresis. Review. *Anal. Chem.* **1975,** *47* (7), 970-983.

49. May, J. C.; McLean, J. A., Ion mobility-mass spectrometry: time-dispersive instrumentation. *Anal. Chem.* **2015,** *87* (3), 1422-1436.

50. Giles, K.; Pringle, S. D.; Worthington, K. R.; Little, D.; Wildgoose, J. L.; Bateman, R. H., Applications of a travelling wave-based radio-frequency-only stacked ring ion guide. *Rapid Commun. Mass Spectrom.* **2004,** *18* (20), 2401-2414.

51. Shvartsburg, A., *Differential mobility spectrometry: nonlinear ion transport and fundamentals of FAIMS*. CRC Press: Boca Raton, 2008.

52. Webb, I. K.; Garimella, S. V.; Tolmachev, A. V.; Chen, T. C.; Zhang, X.; Norheim, R. V.; Prost, S. A.; LaMarche, B.; Anderson, G. A.; Ibrahim, Y. M.; Smith, R. D., Experimental evaluation and optimization of structures for lossless ion manipulations for ion mobility spectrometry with time-of-flight mass spectrometry. *Anal. Chem.* **2014,** *86* (18), 9169-9176.

53. Hamid, A. M.; Ibrahim, Y. M.; Garimella, S. V.; Webb, I. K.; Deng, L.; Chen, T. C.; Anderson, G. A.; Prost, S. A.; Norheim, R. V.; Tolmachev, A. V.; Smith, R. D., Characterization of Traveling Wave Ion Mobility Separations in Structures for Lossless Ion Manipulations. *Anal. Chem.* **2015,** *87* (22), 11301-11308.

54. Fernandez-Lima, F. A.; Kaplan, D. A.; Suetering, J.; Park, M. A., Gas-phase separation using a Trapped Ion Mobility Spectrometer. *Int. J. Ion Mobil. Spectrom.* **2011,** *14* (2-3), 93-98.

55. Fernandez-Lima, F. A.; Kaplan, D. A.; Park, M. A., Note: Integration of trapped ion mobility spectrometry with mass spectrometry. *Rev. Sci. Instr.* **2011,** *82* (12), 126106.

56. Shah, V.; Castro-Perez, J. M.; McLaren, D. G.; Herath, K. B.; Previs, S. F.; Roddy, T. P., Enhanced data-independent analysis of lipids using ion mobility-TOFMSE to unravel quantitative and qualitative information in human plasma. *Rapid Commun. Mass Spectrom.* **2013,** *27* (19), 2195-2200.

57. Damen, C. W.; Isaac, G.; Langridge, J.; Hankemeier, T.; Vreeken, R. J., Enhanced lipid isomer separation in human plasma using reversed-phase UPLC with ion-mobility/high-resolution MS detection. *J. Lipid Res.* **2014,** *55* (8), 1772-1783.

58. Baker, P. R.; Armando, A. M.; Campbell, J. L.; Quehenberger, O.; Dennis, E. A., Three-dimensional enhanced lipidomics analysis combining UPLC, differential ion mobility spectrometry, and mass spectrometric separation strategies. *J. Lipid Res.* **2014,** *55* (11), 2432-2442.

59. Jackson, S. N.; Ugarov, M.; Post, J. D.; Egan, T.; Langlais, D.; Schultz, J. A.; Woods, A. S., A study of phospholipids by ion mobility TOFMS. *J. Am. Soc. Mass Spectrom.* **2008,** *19* (11), 1655-1662.

60. May, J. C.; Goodwin, C. R.; Lareau, N. M.; Leaptrot, K. L.; Morris, C. B.; Kurulugama, R. T.; Mordehai, A.; Klein, C.; Barry, W.; Darland, E.; Overney, G.; Imatani, K.; Stafford, G. C.; Fjeldsted, J. C.; McLean, J. A., Conformational ordering of biomolecules in the gas phase: nitrogen collision cross sections measured on a prototype high resolution drift tube ion mobility-mass spectrometer. *Anal. Chem.* **2014,** *86* (4), 2107-2116.

61. Groessl, M.; Graf, S.; Knochenmuss, R., High resolution ion mobility-mass spectrometry for separation and identification of isomeric lipids. *Analyst* **2015,** *140* (20), 6904-6911.

62. Hines, K. M.; May, J. C.; McLean, J. A.; Xu, L., Evaluation of Collision Cross Section Calibrants for Structural Analysis of Lipids by Traveling Wave Ion Mobility-Mass Spectrometry. *Anal. Chem.* **2016,** *88* (14), 7329-7336.

63. Kim, H. I.; Kim, H.; Pang, E. S.; Ryu, E. K.; Beegle, L. W.; Loo, J. A.; Goddard, W. A.; Kanik, I., Structural characterization of unsaturated phosphatidylcholines using traveling wave ion mobility spectrometry. *Anal. Chem.* **2009,** *81* (20), 8289-8297.

64. Paglia, G.; Angel, P.; Williams, J. P.; Richardson, K.; Olivos, H. J.; Thompson, J. W.; Menikarachchi, L.; Lai, S.; Walsh, C.; Moseley, A.; Plumb, R. S.; Grant, D. F.; Palsson, B. O.; Langridge, J.; Geromanos, S.; Astarita, G., Ion mobility-derived collision cross section as an additional measure for lipid fingerprinting and identification. *Anal. Chem.* **2015,** *87* (2), 1137-1144.

65. Shvartsburg, A. A.; Isaac, G.; Leveque, N.; Smith, R. D.; Metz, T. O., Separation and classification of lipids using differential ion mobility spectrometry. *J. Am. Soc. Mass Spectrom.* **2011,** *22* (7), 1146-1155.

66. Maccarone, A. T.; Duldig, J.; Mitchell, T. W.; Blanksby, S. J.; Duchoslav, E.; Campbell, J. L., Characterization of acyl chain position in unsaturated phosphatidylcholines using differential mobility-mass spectrometry. *J. Lipid Res.* **2014,** *55* (8), 1668-1677.

67. Kyle, J. E.; Zhang, X.; Weitz, K. K.; Monroe, M. E.; Ibrahim, Y. M.; Moore, R. J.; Cha, J.; Sun, X.; Lovelace, E. S.; Wagoner, J.; Polyak, S. J.; Metz, T. O.; Dey, S. K.; Smith, R. D.; Burnum-Johnson, K. E.; Baker, E. S., Uncovering biologically significant lipid isomers with liquid chromatography, ion mobility spectrometry and mass spectrometry. *Analyst* **2016,** *141* (5), 1649-1659.

68. Bowman, A. P.; Abzalimov, R. R.; Shvartsburg, A. A., Broad Separation of Isomeric Lipids by High-Resolution Differential Ion Mobility Spectrometry with Tandem Mass Spectrometry. *J. Am. Soc. Mass Spectrom.* **2017,** *28* (8), 1552-1561.

69. Wojcik, R.; Webb, I. K.; Deng, L.; Garimella, S. V.; Prost, S. A.; Ibrahim, Y. M.; Baker, E. S.; Smith, R. D., Lipid and Glycolipid Isomer Analyses Using Ultra-High Resolution Ion Mobility Spectrometry Separations. *Int. J. Mol. Sci.* **2017,** *18* (1).

70. Jeanne Dit Fouque, K.; Garabedian, A.; Porter, J.; Baird, M.; Pang, X.; Williams, T. D.; Li, L.; Shvartsburg, A.; Fernandez-Lima, F., Fast and Effective Ion Mobility-Mass Spectrometry Separation of d-Amino-Acid-Containing Peptides. *Anal. Chem.* **2017,** *89* (21), 11787-11794.

71. Jeanne Dit Fouque, K.; Salgueiro, L. M.; Cai, R.; Sha, W.; Schally, A. V.; Fernandez-Lima, F., Structural Motif Descriptors as a Way To Elucidate the Agonistic or Antagonistic Activity of Growth Hormone–Releasing Hormone Peptide Analogues. *ACS Omega* **2018,** *3* (7), 7432-7440.

72. Adams, K. J.; Montero, D.; Aga, D.; Fernandez-Lima, F., Isomer Separation of Polybrominated Diphenyl Ether Metabolites using nanoESI-TIMS-MS. *Int. J. Ion Mobil. Spectrom.* **2016,** *19* (2), 69-76.

73. Benigni, P.; Sandoval, K.; Thompson, C. J.; Ridgeway, M. E.; Park, M. A.; Gardinali, P.; Fernandez-Lima, F., Analysis of Photoirradiated Water Accommodated Fractions of Crude Oils

Using Tandem TIMS and FT-ICR MS. *Environ. Sci. Technol.* **2017,** *51* (11), 5978-5988.

74. Benigni, P.; Fernandez-Lima, F., Oversampling Selective Accumulation Trapped Ion Mobility Spectrometry Coupled to FT-ICR MS: Fundamentals and Applications. *Anal. Chem.* **2016,** *88* (14), 7404-7412.

75. Molano-Arevalo, J. C.; Gonzalez, W.; Jeanne Dit Fouque, K.; Miksovska, J.; Maitre, P.; Fernandez-Lima, F., Insights from ion mobility-mass spectrometry, infrared spectroscopy, and molecular dynamics simulations on nicotinamide adenine dinucleotide structural dynamics: NAD(+)vs. NADH. *Phys. Chem. Chem. Phys.* **2018,** *20* (10), 7043-7052.

76. Garabedian, A.; Butcher, D.; Lippens, J. L.; Miksovska, J.; Chapagain, P. P.; Fabris, D.; Ridgeway, M. E.; Park, M. A.; Fernandez-Lima, F., Structures of the kinetically trapped i-motif DNA intermediates. *Phys. Chem. Chem. Phys.* **2016,** *18* (38), 26691-26702.

77. Baglai, A.; Gargano, A. F. G.; Jordens, J.; Mengerink, Y.; Honing, M.; van der Wal, S.; Schoenmakers, P. J., Comprehensive lipidomic analysis of human plasma using multidimensional liquid- and gas-phase separations: Two-dimensional liquid chromatography-mass spectrometry vs. liquid chromatography-trapped-ion-mobility-mass spectrometry. *J. Chromatogr. A.* **2017,** *1530*, 90-103.

78. Zacek, P.; Bukowski, M.; Rosenberger, T. A.; Picklo, M., Quantitation of isobaric phosphatidylcholine species in human plasma using a hybrid quadrupole linear ion-trap mass spectrometer. *J. Lipid Res.* **2016,** *57* (12), 2225-2234.

79. Hernandez, D. R.; Debord, J. D.; Ridgeway, M. E.; Kaplan, D. A.; Park, M. A.; Fernandez-Lima, F., Ion dynamics in a trapped ion mobility spectrometer. *Analyst* **2014,** *139* (8), 1913-1921.

80. McDaniel, E. W.; Mason, E. A., *Mobility and diffusion of ions in gases*. John Wiley and Sons, Inc., New York: New York, 1973; p 381.

81. Tang, K.; Li, F.; Shvartsburg, A. A.; Strittmatter, E. F.; Smith, R. D., Two-dimensional gas-phase separations coupled to mass spectrometry for analysis of complex mixtures. *Anal. Chem.* **2005,** *77* (19), 6381-6388.

82. Garabedian, A.; Baird, M. A.; Porter, J.; Jeanne Dit Fouque, K.; Shliaha, P. V.; Jensen, O. N.; Williams, T. D.; Fernandez-Lima, F.; Shvartsburg, A. A., Linear and Differential Ion Mobility Separations of Middle-Down Proteoforms. *Anal. Chem.* **2018,** *90* (4), 2918-2925.

83. Ekroos, K.; Ejsing, C. S.; Bahr, U.; Karas, M.; Simons, K.; Shevchenko, A., Charting molecular composition of phosphatidylcholines by fatty acid scanning and ion trap MS3 fragmentation. *J. Lipid Res.* **2003,** *44* (11), 2181-2192.